Supporting Information

A Cross-like Hierarchical Porous Lithium-rich Layered Oxide with (110)-oriented Crystal Plane as High Energy Density Cathode for Lithium Ion Batteries

Min Chen[a], Xiaojing Jin[c], Zhi Chen[a], Yaotang Zhong[a], Youhao Liao[a,b], Yongcai Qiu[a,b,c], Guozhong Cao[d],* Weishan Li [a,b*]

a. School of Chemistry and Environment, South China Normal University, Guangzhou 510006, China

b. National and Local Joint Engineering Research Center of MPTES in High Energy and Safety LIBs, Engineering Research Center of MTEES (Ministry of Education), and Key Lab. of ETESPG(GHEI), South China Normal University, Guangzhou 510006, China

c. School of Environment and Energy, South China University of Technology, Guangzhou 510006 China

d. Department of Materials Science and Engineering, University of Washington, Seattle, Washington 98195, United States.

* Corresponding authors, email: gzcao@u.washington.edu; liwsh@scnu.edu.cn.

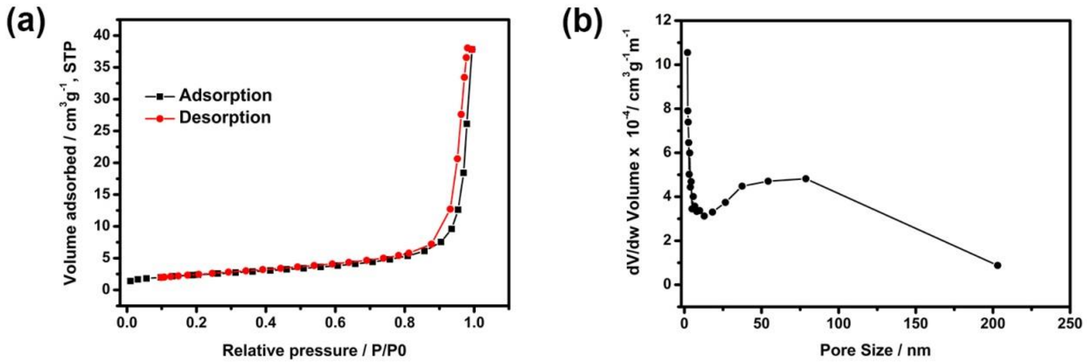

Figure S1. Nitrogen adsorption and desorption isotherm (a) and corresponding pore size distribution curve (b) of CHP-LMNO.

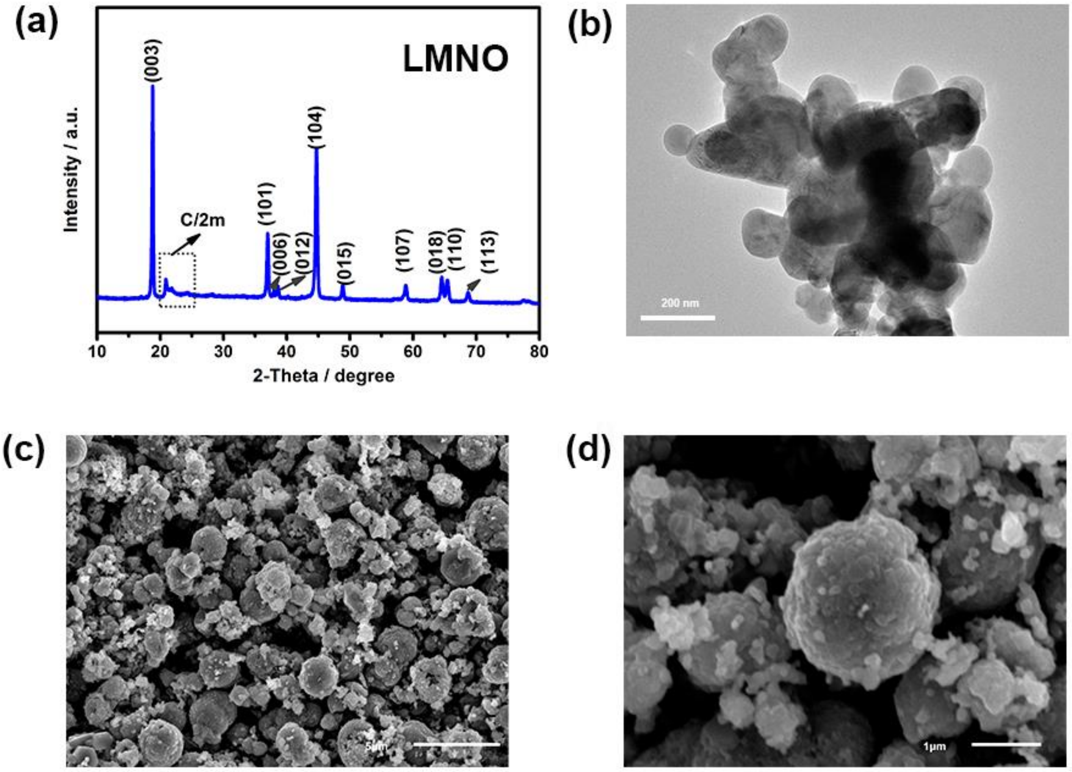

Figure S2. (a) XRD pattern, (b) TEM, (c) SEM, and (d) magnified SEM images of LMNO.

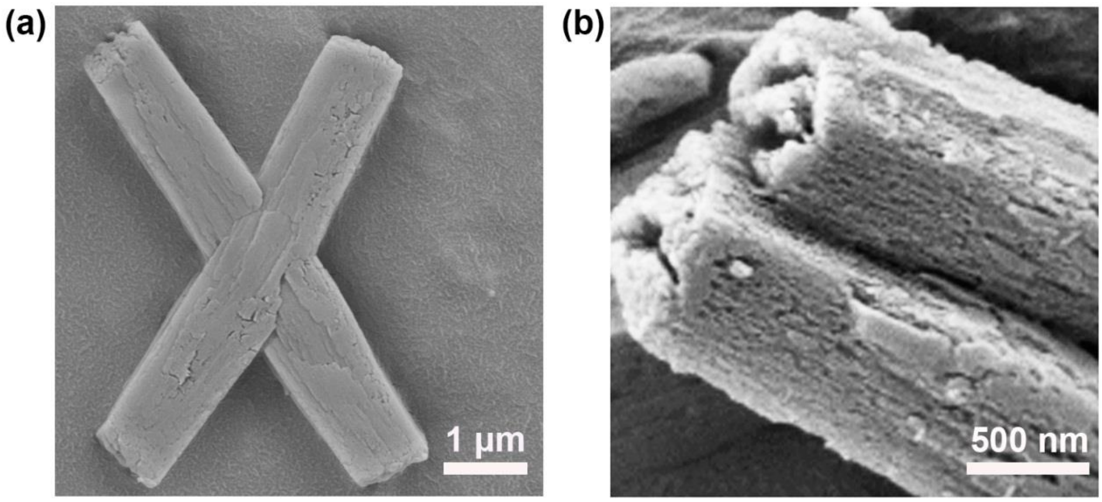

Figure S3. (a) SEM image and (b) local magnified SEM image of manganese-nickel oxalate precursor.

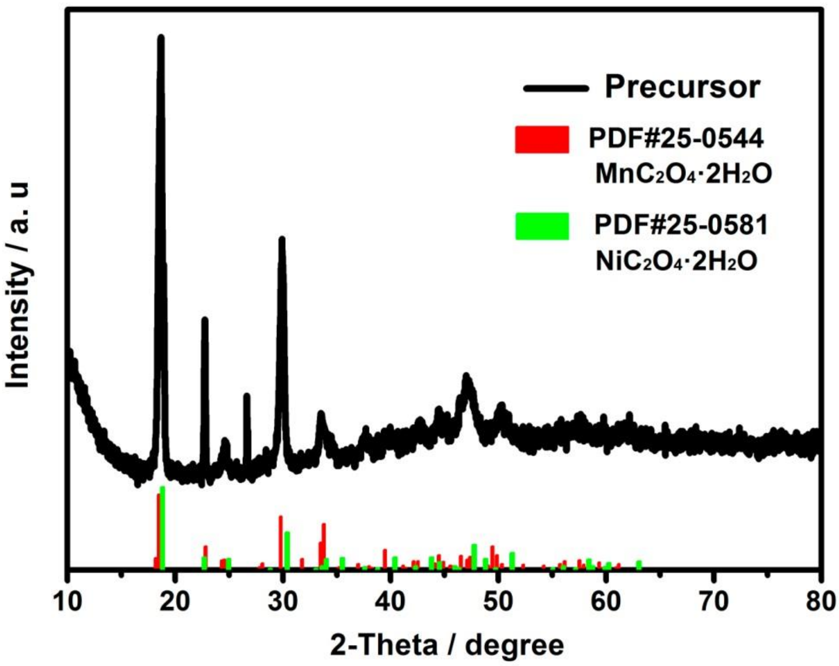

Figure S4. XRD pattern of manganese-nickel oxalate precursor.

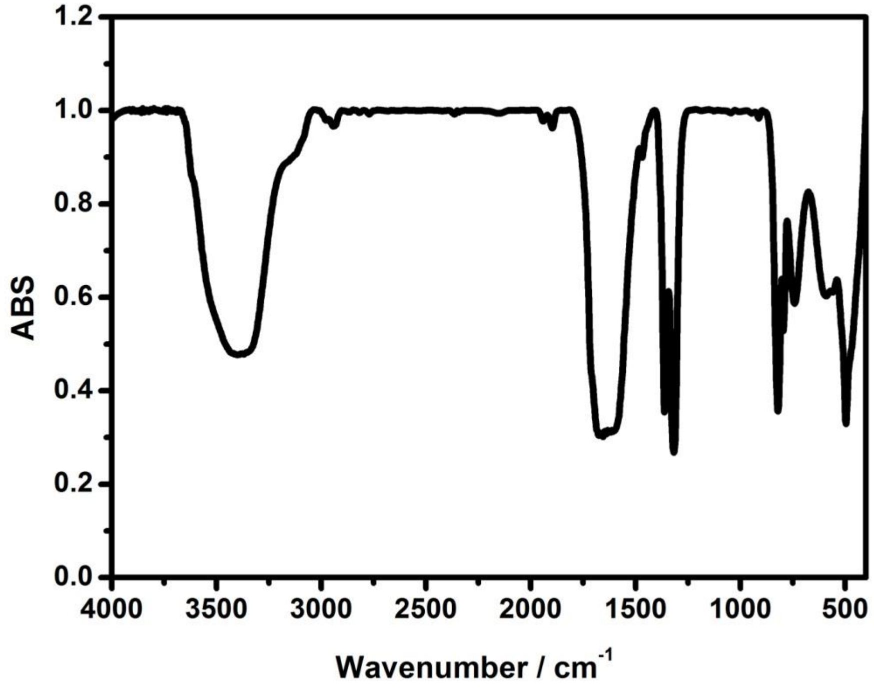

Figure S5. FTIR spectrum of manganese-nickel oxalate precursor.

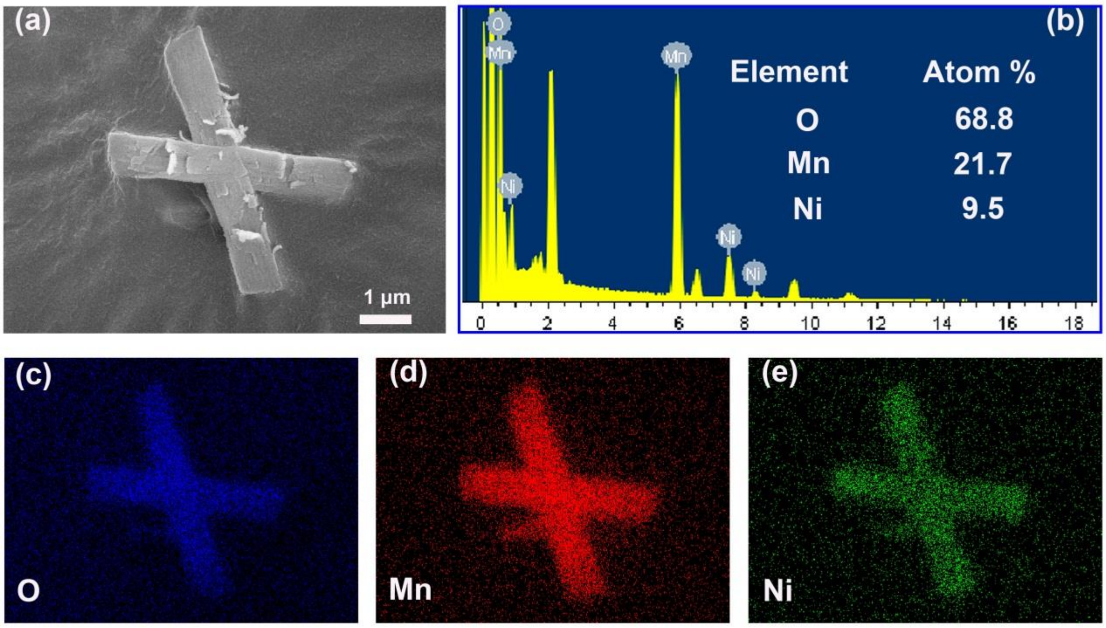

Figure S6. (a) SEM image of manganese-nickel oxide, (b) EDS pattern and the element content, and (c, d and e) element mappings of manganese-nickel oxide.

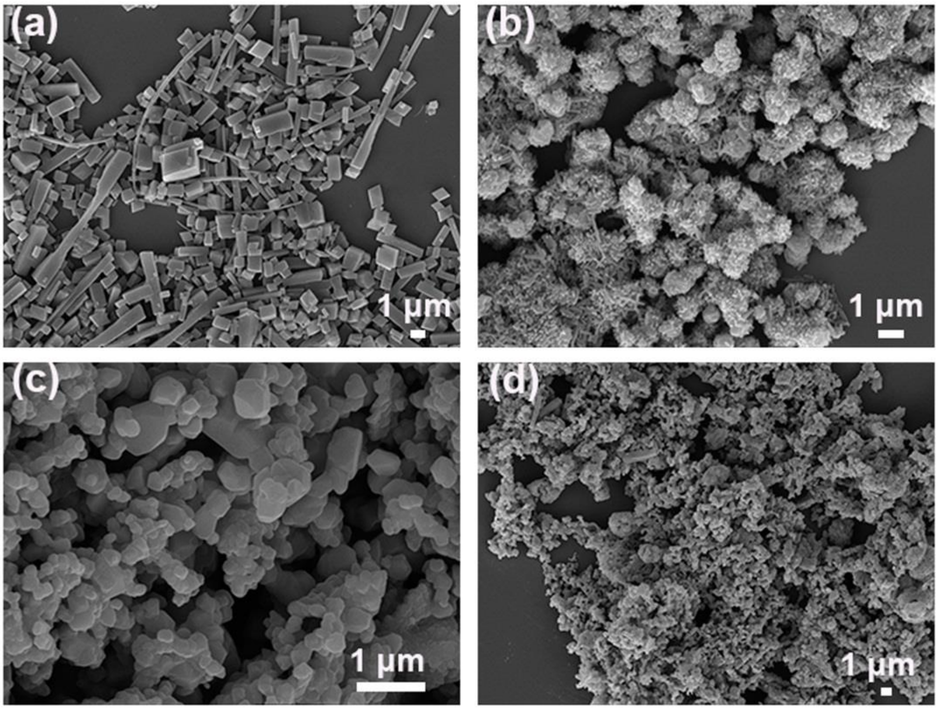

Figure S7. (a, c) SEM images of the manganese oxalate precursor and its oxide, (b, d) SEM images of the nickel oxalate precursor and its oxide.

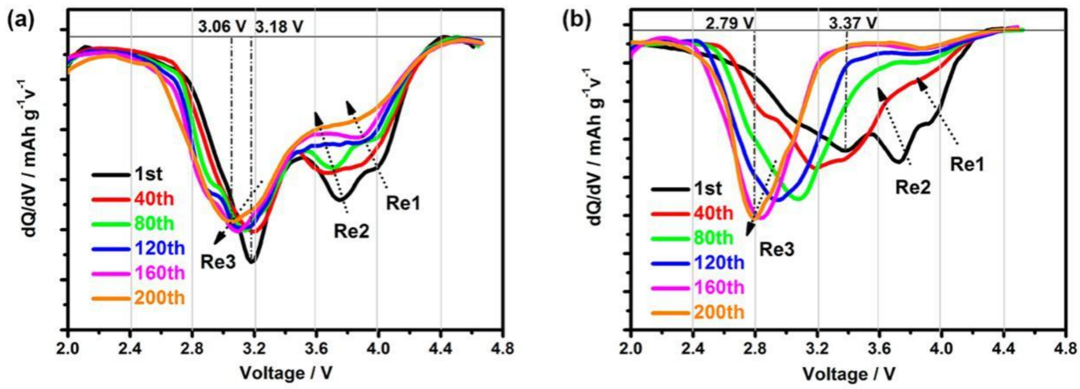

Figure S8. dQ/dV plots of (a) CHP-LMNO and (b) LMNO at various cycles.

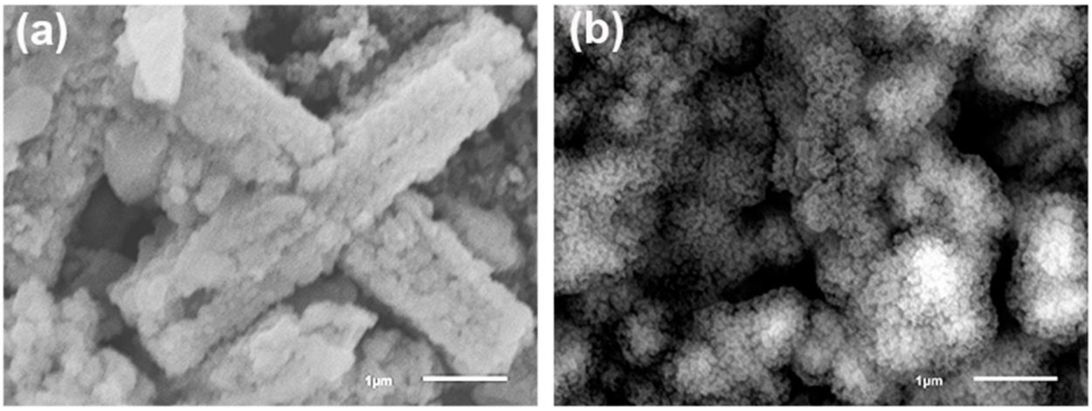

Figure S9. SEM images of (a) CHP-LMNO and (b) LMNO after 200 cycles.

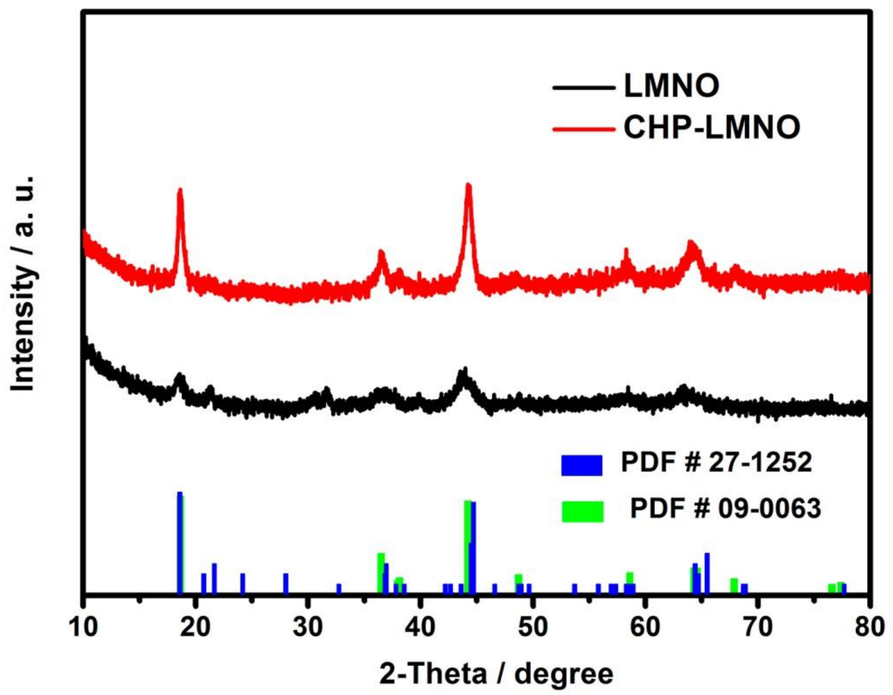

Figure S10. XRD patterns of CHP-LMNO and LMNO after 200 cycles.

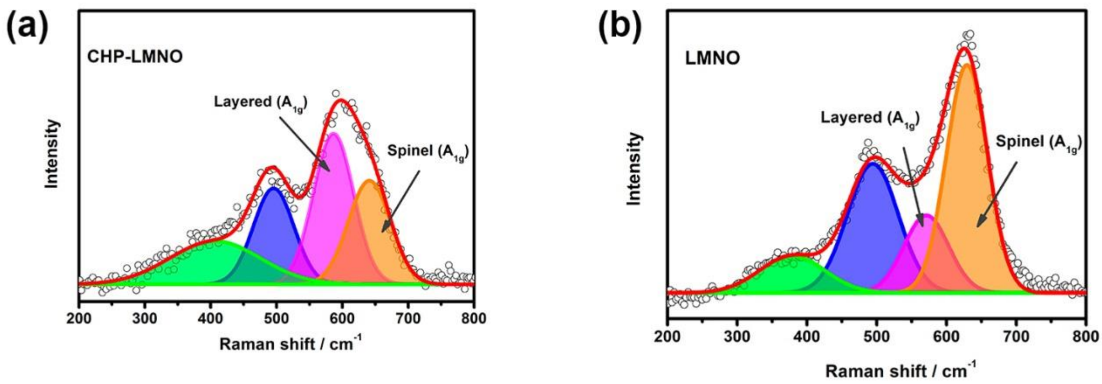

Figure S11. Raman spectra of CHP-LMNO and LMNO after 200 cycles.

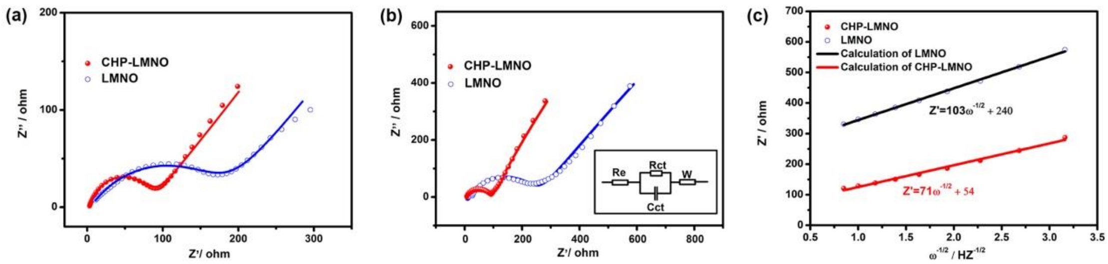

Figure S12. EIS plots (a) after 10 and (b) 200 cycles at 0.5 C; (c) profiles of Z' vs. $\omega^{-1/2}$ from 1 to 0.1 Hz for CHP-LMNO and LMNO.

Electrochemical impedance spectroscopy (EIS) was used to confirm the accelerated kinetics, which was performed at the full lithium inserted state (2 V). Figure S12 presents the impedance spectra of the electrodes after 10 and 200 cycles. These spectra are composed of two parts: an arc at high frequencies corresponding interface impedance between materials and electrolyte, and a slope line at low frequencies reflecting the Warburg impedance for lithium ion diffusion,[1-3] and can be well fitted by the equivalent circuit in Figure S12b. The fitting results are presented in Table S2. After 10 cycles (Figure S12a), the interface resistance of CHP-LMNO and LMNO is about 80 Ω and 179 Ω, respectively, suggesting that CHP-LMNO has a fast lithium intercalation/de-intercalation kinetics. After 200 cycles, the interface resistance keeps almost unchanged for CHP-LMNO, but increases significantly to 239 Ω for LMNO, illustrating the far stable structure of CHP-LMNO than LMNO. Meanwhile, the lithium diffusion coefficient can be estimated by the slope (σ) of linear relation of the impedance with the frequency in Figure S12c based on:

$$D_{Li^+} = R^2T^2/2n^4A^2F^4C^2\sigma$$

where R is the ideal gas constant, T is the absolute temperature, n is the number of electron per molecule, A is the surface area of the electrode, F is the Faraday constant, C is the concentration of Li^+ in active material that is determined by its lithium-inserted state, and σ is the Warburg factor.[1, 4] The lithium diffusion coefficient is 5.2×10^{-13} cm^2 s^{-1} for CHP-LMNO and 4.6×10^{-14} cm^2 s^{-1} for LMNO, indicating fast transportation of Li^+ in CHP-LMNO than LMNO.

Table S1. Chemical compositions determined by ICP and crystal lattice parameters determined by XRD

Samples	Composition		Lattice parameter		
	Target product	ICP-AES	α / Å	c / Å	c/α
CHP-LMNO	$Li_{1.2}Mn_{0.6}Ni_{0.2}O_2$	$Li_{1.167}Mn_{0.583}Ni_{0.250}O_2$	2.8654	14.2865	4.9858
LMNO	$Li_{1.2}Mn_{0.6}Ni_{0.2}O_2$	$Li_{1.172}Mn_{0.586}Ni_{0.242}O_2$	2.8643	14.2578	4.9777

Table S2. Fitting parameters for electrochemical impedance spectra after 200 cycles

Samples	R_e(Ω)	R_{ct}(Ω)	R_{total}(Ω)	D_{Li^+}(cm^2 s^{-1})
CHP-LMNO	4.0	86.0	90.0	5.2×10^{-13}
LMNO	8.0	239.0	247.0	4.6×10^{-14}

Table S3. Comparison in electrochemical performances

Morphology	**Voltage window / V**	**Current density / mA g^{-1}**	**Discharge capacity**	**Ref.**
Hollow porous bowl-shape	2.0-4.8	4000	103.6	5
Olive-like with micro/nano structure	2.0-4.6	2500	142.8	6
Hollow porous hierarchical-structure	2.0-4.8	2000	162.6	7
Porous nanorods	2.0-4.8	1000	145.4	8
Nanowires	2.0-4.8	2800	256	9
Micro- and nanostructured bars	2.0-4.8	2500	151	10
Uniform nanoparticles	3.0-4.8	263	130	11
Hierarchical plate-like	2.0-4.8	1000	204	12
Hierarchically porous micro-rod	2.0-4.8	1250	172.7	13
Peanut-like hierarchical micro/nano structure	2.0-4.8	2000	145	14
Microrods	2.0-4.8	1600	150.6	15
Three-dimensional fusiform hierarchical micro/nano structure	2.0-4.8	1000	166.8	16
Hollow sphere	2.0-4.8	1000	138.1	17
Nanoarchitecture multi-structure	2.0-4.6	250	200	18
Microstructure	2.0-4.8	3200	171	19
Mesoporous foams	2.0-4.8	200	208	20

Morphology	**Voltage window / V**	**Current density / mA g^{-1}**	**Discharge capacity**	**Ref.**
Hierarchical nanoplates	2.0-4.8	5000	141.7	21
octahedral core-shell like	2.0-4.8	2000	162.4	22
Microsphere	2.0-4.6	1200	185.1	23
Three-dimensional nanoporous structure	2.0-4.8	1250	197.6	24
A cross-like hierarchical porous structure	2.0-4.8	5000 25	143 276	Our work

Supplementary References

1. M. Chen, D. Chen, Y. Liao, X. Zhong, W. Li and Y. Zhang, *ACS Appl. Mater. Interfaces*, 2016, **8**, 4575-4584.
2. M. Chen, X. Xiang, D. Chen, Y. Liao, Q. Huang and W. Li, *J. Power Sources*, 2015, **279**, 197-204.
3. G. Wang, L. Yi, R. Yu, X. Wang, Y. Wang, Z. Liu, B. Wu, M. Liu, X. Zhang, X. Yang, X. Xiong and M. Liu, *ACS Appl. Mater. Interfaces*, 2017, **9**, 25358-25368.
4. J. Zeng, Y. Cui, D. Qu, Q. Zhang, J. Wu, X. Zhu, Z. Li and X. Zhang, *ACS Appl. Mater. Interfaces*, 2016, **8**, 26082-26090.
5. Y. Zhang, W. Zhang, S. Shen, X. Yan, A. Wu, J. Yin and J. Zhang, *J. Power Sources*, 2018, **380**, 164-173.
6. G. Wang, L. Yi, R. Yu, X. Wang, Y. Wang, Z. Liu, B. Wu, M. Liu, X. Zhang, X. Yang, X. Xiong and M. Liu, *ACS Appl. Mater. Interfaces*, 2017, **9**, 25358-25368.
7. F. Fu, J. Tang, Y. Yao and M. Shao, *ACS Appl. Mater. Interfaces*, 2016, **8**, 25654-25659.
8. D. Chen, Q. Yu, X. Xiang, M. Chen, Z. Chen, S. Song, L. Xiong, Y. Liao, L. Xing and W. Li, *Electrochim. Acta*, 2015, **154**, 83-93.
9. M. G. Kim, M. Jo, Y. S. Hong and J. Cho, *Chem. Commun.*, 2009, **2**, 218-220.
10. G. Ma, S. Li, W. Zhang, Z. Yang, S. Liu, X. Fan, F. Chen, Y. Tian, W. Zhang, S. Yang and M. Li, *Angew. Chem. Int. Ed.*, 2016, **55**, 3667-3671.

11. X. Xiang, X. Li and W. Li, *J. Power Sources*, 2013, **230**, 89-95.

12. J. Zeng, Y. Cui, D. Qu, Q. Zhang, J. Wu, X. Zhu, Z. Li and X. Zhang, *ACS Appl. Mater. Interfaces*, 2016, **8**, 26082-26090.

13. L. Zhang, W. Borong, L. Ning and W. Feng, *Electrochim. Acta*, 2014, **118**, 67-74.

14. Y.-D. Zhang, Y. Li, X.-Q. Niu, D.-H. Wang, D. Zhou, X.-L. Wang, C.-D. Gu and J.-P. Tu, *J. Mater. Chem. A*, 2015, **3**, 14291-14297.

15. F. Fu, Y. Yao, H. Wang, G.-L. Xu, K. Amine, S.-G. Sun and M. Shao, *Nano Energy*, 2017, **35**, 370-378.

16. Y. Li, Y. Bai, C. Wu, J. Qian, G. Chen, L. Liu, H. Wang, X. Zhou and F. Wu, *J. Mater. Chem. A*, 2016, **4**, 5942-5951.

17. W. Ding, X. Cui, J. Lei, X. Lin, S. Zhao, Q.-H. Wu, M. Zheng and Q. Dong, *Electrochim. Acta*, 2018, **264**, 260-268.

18. D. Wang, I. Belharouak, G. Zhou and K. Amine, *Adv. Fun. Mater.*, 2013, **23**, 1070-1075.

19. W. Hua, M. Chen, B. Schwarz, M. Knapp, M. Bruns, J. Barthel, X. Yang, F. Sigel, R. Azmi, A. Senyshyn, A. Missiul, L. Simonelli, M. Etter, S. Wang, X. Mu, A. Fiedler, J. R. Binder, X. Guo, S. Chou, B. Zhong, S. Indris and H. Ehrenberg, *Adv. Energy Mater.*, 2019, **9**, 1803094.

20. Y. Jiang, Z. Yang, W. Luo, X.-L. Hu, W.-X. Zhang and Y.-H. Huang, *J. Mater. Chem.*, 2012, **22**, 14964.

21. L. Chen, Y. Su, S. Chen, N. Li, L. Bao, W. Li, Z. Wang, M. Wang and F. Wu,

Adv. Mater., 2014, **26**, 6756-6760.

22. W. He, J. Liu, W. Sun, W. Yan, L. Zhou, C. Wu, J. Wang, X. Yu, H. Zhao, T. Zhang and Z. Zou, *ACS Appl. Mater. Interfaces*, 2018, **10**, 23018-23028.

23. D. Luo, G. Li, C. Fu, J. Zheng, J. Fan, Q. Li and L. Li, *Adv. Energy Mater.*, 2014, **4**, 1400062.

24. B. Qiu, C. Yin, Y. Xia and Z. Liu, *ACS Appl. Mater. Interfaces*, 2017, **9**, 3661-3666.